

Explaining the Adaptive Generalisation Gap

Diego Granziol

Samuel Albanie

Xingchen Wan

Stephen Roberts

University of Oxford

Abstract

We conjecture that the reason for the difference in generalisation between adaptive and non-adaptive gradient methods stems from the failure of adaptive methods to account for the greater levels of noise associated with flatter directions in their estimates of local curvature. This conjecture—motivated by results in random matrix theory [1, 2]—has implications for optimisation in both simple convex settings and deep neural networks. We demonstrate that typical schedules used for adaptive methods (with low numerical stability or damping constants) serve to bias relative movement towards flat directions relative to sharp directions, effectively amplifying the noise-to-signal ratio and harming generalisation. We show that the numerical stability/damping constant used in these methods can be decomposed into a learning rate reduction and linear shrinkage of the estimated curvature matrix. We then demonstrate significant generalisation improvements by increasing the shrinkage coefficient, closing the generalisation gap entirely in our neural network experiments. Finally, we show that other popular modifications to adaptive methods, such as decoupled weight decay [3] and partial adaptivity [4] can be shown to calibrate parameter updates to make better use of sharper, more reliable directions.

1 Introduction

The success of deep neural networks across a wide variety of tasks, from speech recognition to image classification, has drawn wide-ranging interest in their optimisation. *Adaptive gradient* optimisers, which alter the per parameter learning rate depending on historical gradi-

ent information, lead to significantly faster convergence of the training loss than non adaptive methods, such as stochastic gradient descent (SGD) with momentum [5]. Popular examples include Adam [6], AdaDelta [7] and RMSprop [8]. However, for practical applications the final test set results are more important than the training performance. The difference between training and test performance is known as the *generalisation gap*. For many image and language problems of interest, the test set performance of adaptive gradient methods is significantly worse than SGD [9]—a phenomenon that we refer to as the *adaptive generalisation gap*. As a consequence of this effect, many state-of-the-art models, especially for image classification datasets such as CIFAR [10] and ImageNet [11, 12], are still trained using SGD with momentum.

Although less widely used, another class of adaptive methods which suffer from the same phenomenon are *stochastic second order methods*, which seek to alter the learning rate along the eigenvectors of the second derivative of the loss function. KFAC [13] uses a Kronecker factored approximation of the Fisher information matrix (which can be seen as a positive definite approximation to the Hessian [14]). Other methods use Hessian-vector products [15, 16] in conjunction with Lanczos/Conjugate gradients [17] (which can be seen as a low rank approximation to the Hessian). Despite strong performance on certain complex tasks such as deep auto-encoders [18], their test performance on large-scale image problems is also lower than that of SGD [19].

In this paper we argue that adaptive methods are over-confident in their updates in the flattest directions of the loss. We show that this is sub-optimal in terms of optimising the true loss and hence harms generalisation performance. We demonstrate this empirically in an online convex example, where we actively perturb the sharp directions, reducing generalisation without impacting training. We also demonstrate this implicitly for large neural networks by altering the damping/stability constant, which we show alters effective learning rate ratio between the sharp and flat directions.

Given the benefits of adaptive methods (such as swifter convergence and reduced sensitivity to hyper-parameters relative to SGD), understanding the adaptive generalisation gap has significant implications. In this work we show that altering the numerical stability constant in Adam [20] can be interpreted as an approximation to linear shrinkage of the noisy Hessian (enabling for reduction of mean square error [21]). We further show that many heuristics used to improve generalisation of these methods, such as directly implementing weight decay instead of $L2$ regularisation [3], or altering the power in the denominator of the Adam algorithm [4] can be interpreted within our framework: they correct for the curvature estimation bias and increase relative movement in favour of sharp directions during the optimisation trajectory.

1.1 Related Work

Prior theoretical work on generalisation has investigated the correlation between the learning rates to batch size ratio and generalisation during SGD optimisation [22] along with stability analysis to show that larger learning rates lead to lower spectral norms (which should generalise better according to Bayesian and minimum description length principles [23]). Li et al. [24] argue that larger learning rates learn “hard to generalise, easy to fit patterns” better than their lower learning rate counterparts and that this forms part of the generalisation gap. However, to the best of our knowledge, there has been no theoretical work analysing the *adaptive generalisation gap*, with the notable exception of Wilson et al. [9], who consider the poor generalisation performance of adaptive methods to be inherent (and show this on a simple example).

Practical amendments to improve generalisation of adaptive methods have included dynamically switching between Adam and SGD [25] and altering the preconditioning matrix in Adam by introducing a free parameter $p \in [0, 1/2]$, where instead of taking the square root of the second moment of the parameter gradient, the p ’th power is taken [4]. This toggles between Adam and SGD¹. The choice of $0 \leq p \leq 1/4$ has been shown to have improved convergence properties to that of AMSgrad [26]. Another recent popular amendment has been implementing weight decay instead of $L2$ regularisation (which are not equivalent for adaptive methods) [3]. Zhang et al. [27], investigate the effect of implementing decoupled weight decay for KFAC and similarly note increased generalisation performance. Choi et al. [20] show that by altering the damping or numerical stability constant, typically taken as 10^{-8} in Adam, Adam can simulate SGD and retain its generalisation

performance.

While empirically effective, these alterations lack a clear theoretical motivation. Neither [25], [20], [3] nor [4] explain why Adam (or adaptive methods in general) inherently generalises worse than SGD. Instead, they show that switching from Adam to SGD, or making Adam more similar to SGD brings improvements. A clear analysis of how SGD differs from adaptive methods and why this impacts generalisation is not provided in any of the aforementioned works.

1.2 Contributions

In this paper we conjecture that a key driver of the adaptive generalisation gap is the fact that adaptive methods *fail to account for the greater levels of noise associated with their estimates of flat directions in the loss landscape*. The fundamental principle underpinning this conjecture—that sharp directions contain information from the underlying process and that flat directions are largely dominated by noise—is theoretically motivated from the spiked covariance model [28]. This model has been successfully applied in Principal Component Analysis (PCA), covariance matrix estimation and finance [29, 30, 2, 31]. We revisit this idea in the context of deep neural network optimisation by defining the *estimated curvature learning rate ratio*:

$$\mathcal{R}_{\text{est-curv}} := \frac{\alpha_{\text{flat}}}{\alpha_{\text{sharp}}} \quad (1.1)$$

where α_{flat} and α_{sharp} are the learning rates along the flat and sharp directions, respectively and this ratio encapsulates the noise-to-signal ratio as motivated by our conjecture (the terms *flat* and *sharp* are defined more precisely in Sec. 2.1). We study the role of $\mathcal{R}_{\text{est-curv}}$ on both logistic regression with the MNIST dataset and Deep Neural Networks such as the VGG-16 on the CIFAR-100 dataset. Our results indicate that typical hyper-parameter settings for adaptive methods produce a systematic bias in favour of an $\mathcal{R}_{\text{est-curv}}$ that is too large and that this is a contributing factor in the adaptive generalisation gap. We then demonstrate that increasing the damping or numerical stability constants in adaptive methods can be seen as an amalgamation of learning rate reduction and linear shrinkage of the implicit Hessian/covariance of gradients matrix. One consequence of this result is that it provides theoretical justification for the practice of *epsilon tuning* [20] in typical optimisation routines. Our framework further provides insight into modern developments in improving generalisation of adaptive algorithms, namely *decoupled weight decay* [3] and *partial adaptivity* [4]. Each of these methods effectively decreases $\mathcal{R}_{\text{est-curv}}$, correcting for the bias.

¹ $p = 1/2$ reduces to Adam and $p = 0$ reduces to SGD with learning rate $\alpha/1 + \epsilon$.

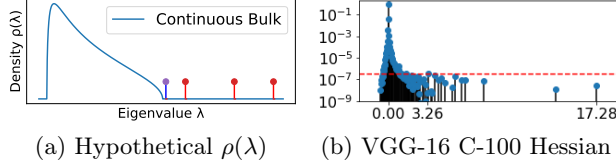


Figure 1: (a) shows a Hypothetical spectral density plot where we have a continuous bulk with sharp support, a finite size fluctuation (shown in blue) which corresponds to the Tracy-Widom region and three well-separated outliers (shown in red). (b) VGG-16 Hessian $\mathbf{H} \in \mathbb{R}^{P \times P}$ on the CIFAR-100 dataset at epoch 150. The red dotted line corresponds to κ/P , where $P = 1.6 \times 10^7$ and $\kappa = 5$, which is taken as an approximate threshold defining the boundary of the bulk.

Paper Structure: In Sec. 2 below, we first describe the theory that motivates our generalisation conjecture. In Sec. 3 we introduce adaptive optimisers and how our conjecture relates to their generalisation performance. We provide empirical evidence to support our claims in Sections 4 and 5. Finally, we relate our conjecture to several widely-used optimisation techniques in Sec. 6.

2 The Spiked Covariance Model, Outliers, and the True Loss

Covariance cleaning considers the problem of how a covariance matrix $\mathbf{H} \in \mathbb{R}^{P \times P}$ differs under the expectation of the data generating distribution (true covariance matrix) from its empirical average using N samples (the empirical covariance matrix). In the limit $N \rightarrow \infty$ for finite P , by the central limit theorem the empirical estimator converges to the true. However when $q = P/N > 0$, the deviations can be significant [2]. The spectral perturbations due to this limited sampling can be characterised analytically by assuming the perturbation to be the addition or multiplication of a random matrix [32], which we refer to as the *noise matrix*. The difference between the empirical covariance matrix and the true covariance matrix is entirely dependent on the interaction between the eigenvalue/eigenvector pairs of the true covariance matrix with those of the noise matrix. Many adaptive gradient methods form an online approximation to the gradient covariance and hence these perturbations are relevant to their generalisation. For stochastic second order methods, [33] extends these ideas to formally include the Hessian of neural networks. In the next section we argue that the eigenvectors corresponding to the eigenvalues of largest magnitude are least affected and hence most accurately estimated.

2.1 Intuition: Why Sharp directions retain more information than Flat ones

The spectrum of the noise matrix occupies a continuous region (sharp in the asymptotic limit [2]) known as *bulk* supported between $[\lambda_-, \lambda_+]$ [2, 31, 21] (shown in Fig. 1a). A bulk region has also been observed in deep learning [34, 35, 36]. Within this bulk all information about the original eigenvalue/eigenvector pairs is lost [1] (these eigenvectors are uniformly distributed on the unit sphere [32]). We define any eigenvalue $\lambda_i \leq \lambda_+$ as *flat*. For finite-size samples and network size, there exists a region beyond the predicted asymptotic support of the noise matrix, called the Tracy-Widom region [37, 38], where there may be isolated eigenvalues which are part of the noise matrix spectrum (also shown in Fig. 1a). Anything beyond the Tracy-Widom region $\lambda_i \gg \lambda_+$ (typically in the literature only semi positive definite matrices are considered, but it is simple to extend the arguments to negative outliers $\lambda_i \ll \lambda_-$), is considered an outlier and corresponds to a *sharp* direction. *Such directions represent underlying structure from the true data.* The eigenvectors corresponding to these eigenvalues can be shown to lie in a cone around their true values [32]. In Figure 1b, we show the Hessian at the 150'th epoch of the VGG-16. Here, similar to our hypothetical example, we see a continuous region, followed by a number of eigenvalues which are close to (but not within) the bulk, and finally, several clear outliers.

2.2 Notation

For an input, output pair $\mathbf{x} \in \mathbb{R}^{d_x}$, $\mathbf{y} \in \mathbb{R}^{d_y}$ and a given prediction function $h(\cdot; \cdot) : \mathbb{R}^{d_x} \times \mathbb{R}^P \rightarrow \mathbb{R}^{d_y}$, we consider the family of prediction functions parameterised by a weight vector \mathbf{w} , i.e., $\mathcal{H} := \{h(\cdot; \mathbf{w}) : \mathbf{w} \in \mathbb{R}^P\}$ with loss function $\ell(h(\mathbf{x}; \mathbf{w}), \mathbf{y}) : \mathbb{R}^{d_x} \times \mathbb{R}^{d_y} \rightarrow \mathbb{R}$. The loss over our data generating distribution $\psi(\mathbf{x}, \mathbf{y})$ (often referred to as the *true loss*) is:

$$L_{true}(\mathbf{w}) = \int \ell(h(\mathbf{x}; \mathbf{w}), \mathbf{y}) d\psi(\mathbf{x}, \mathbf{y}) \quad (2.1)$$

with corresponding gradient $\nabla R_{true}(\mathbf{w})$ and Hessian $\mathbf{H}_{true}(\mathbf{w}) = \nabla^2 R_{true}(\mathbf{w}) \in \mathbb{R}^{P \times P}$. In practice, given a finite dataset of size N , we only have access to the *empirical loss*

$$L_{emp}(\mathbf{w}) = \frac{1}{N} \sum_{i=1}^N \ell(h(\mathbf{x}_i; \mathbf{w}), \mathbf{y}_i) \quad (2.2)$$

with empirical gradient $\nabla R_{emp}(\mathbf{w})$ and empirical Hessian $\mathbf{H}_{emp}(\mathbf{w}) = \nabla^2 R_{emp}(\mathbf{w})$. To further reduce com-

putation cost, typically the batch loss

$$L_{batch}(\mathbf{w}) = \sum_{i=1}^B \ell(h(\mathbf{x}_i; \mathbf{w}), \mathbf{y}_i) / B, \text{ where } B \ll N \quad (2.3)$$

and the gradients $\mathbf{g}_{batch}(\mathbf{w})$ and Hessians $\mathbf{H}_{batch}(\mathbf{w})$ are employed. Weight vectors which achieve low values of Equation 2.2 do not necessarily achieve low values of Equation 2.1 (producing a generalisation gap). In this paper although we optimise with respect to the cross entropy loss, we follow the common practice of assessing generalisation via the classification accuracy.

2.3 Key Result

We highlight a particular insight from the spiked covariance literature [39] which implies that *sharper directions are estimated more accurately than flatter directions*. This statement is characterised more precisely by the following theorem in [33] (which holds under the conditions stated in the suppl. material, with full proof in [32]):

Theorem 1. *The eigenvector overlap between the eigenvectors $\hat{\phi}_i \in \mathbb{R}^{P \times 1}$ of the Hessian of the mini-batch $\nabla^2 L_{batch}(\mathbf{w}_k)$ of batch size B and the eigenvectors ϕ_i of the Hessian under the expectation of the true data distribution $\nabla^2 L_{true}(\mathbf{w}_k)$, where $L_{true}(\mathbf{w}_k) = \int \ell(\mathbf{w}_k; \mathbf{x}, \mathbf{y}) d\psi_{\mathbf{x}, \mathbf{y}}$ is given by*

$$|\hat{\phi}_i^T \phi_i|^2 = \begin{cases} 1 - \frac{P\sigma^2}{B\lambda_i^2} & \text{if } |\lambda_i| > \sqrt{\frac{P}{B}}\sigma, \\ 0 & \text{otherwise,} \end{cases} \quad (2.4)$$

where σ captures the sampling noise per Hessian element for a single sample.

To summarise: the key takeaway of this result is that *sharper directions possess a better signal-to-noise ratio than flatter directions in estimating the true loss surface*. This effect is important for adaptive methods which rely on curvature estimation (either explicitly for stochastic second order methods or implicitly for adaptive gradient methods) to accelerate their progress on the true loss surface.

In the next section, we provide empirical evidence that as we increase the *estimated curvature learning rate ratio* in the flat-to-sharp directions $\mathcal{R}_{est-curv}$, generalisation indeed suffers (lending $\mathcal{R}_{est-curv}$ a loose interpretation as a noise-to-signal ratio). It is interesting to note that in the original Adam paper [6], the authors offer an interpretation of the square root of Adam’s diagonal approximation to the covariance of gradients matrix as the noise component in a signal-to-noise ratio. Our work suggests that this does not quite capture the full picture—a further correction term is required to

prevent adaptive gradient methods from exhibiting a bias towards a greater $\mathcal{R}_{est-curv}$ value than desired. We quantify this statement, and its relationship to linear shrinkage, more precisely in Sec. 3.2. In fact we experimentally show in Sec. 5.2 that by increasing the movement along precisely these high variance directions that generalisation performance improves even beyond that of SGD.

3 Adaptive Optimisation

Consider a general iterative optimiser that seeks to minimise the scalar loss $L(\mathbf{w})$ for a set of model parameters $\mathbf{w} \in \mathbb{R}^P$. The $k+1$ -th iteration of such an optimiser can be written² as follows:

$$\mathbf{w}_{k+1} \leftarrow \mathbf{w}_k - \alpha \mathbf{B}^{-1} \nabla L_{batch}(\mathbf{w}_k) \quad (3.1)$$

where α is the global learning rate. For SGD, $\mathbf{B} = \mathbf{I}$ whereas for adaptive methods, \mathbf{B} typically provides some form of approximation to the Hessian $\mathbf{B} \approx \nabla^2 L_{batch}(\mathbf{w}_k)$. To take a prominent example, Adam uses the square root of the moving uncentered second moment of the per-parameter gradient [6] that can be interpreted as a running diagonal approximation to the covariance of gradients. It has been argued that this is close to the Hessian for DNNs [40, 22, 41, 42, 43]. Other methods use Hessian-vector products, using either Lanczos or conjugate gradient techniques [17] to approximate $\mathbf{B}^{-1} \nabla L_{batch}(\mathbf{w}_k)$ [16, 15] (which for a number of products $m \ll P$ can be seen as a low rank inverse approximation to \mathbf{B}) or direct inversion of Kronecker factored approximations [13].

Writing this update in the eigenbasis of the Hessian³ $\mathbf{H} = \nabla^2 L_{batch}(\mathbf{w}_k) = \sum_i^P \lambda_i \phi_i \phi_i^T \in \mathbb{R}^{P \times P}$, where $\lambda_1 \geq \lambda_2 \geq \dots \geq \lambda_P \geq 0$ represent the ordered scalar eigenvalues, the parameter step takes the form:

$$\mathbf{w}_{k+1} = \mathbf{w}_k - \sum_{i=1}^P \frac{\alpha}{\lambda_i + \delta} \phi_i \phi_i^T \nabla L(\mathbf{w}_k). \quad (3.2)$$

Here, δ is a damping (or numerical stability) term. This damping term, which is typically grid searched [15] or adapted during training [13], can be interpreted as a trust region [15] that is required to stop the optimiser moving too far in directions deemed flat ($\lambda_i \approx 0$) and diverging. In Adam [6], it is set to 10^{-8} . For small values of δ , α must also be small to avoid optimisation instability, hence global learning rates and damping are coupled in adaptive optimisers.

²Ignoring additional features such as momentum and explicit regularisations.

³We assume this to be positive definite or that we are working with a positive definite approximation thereof.

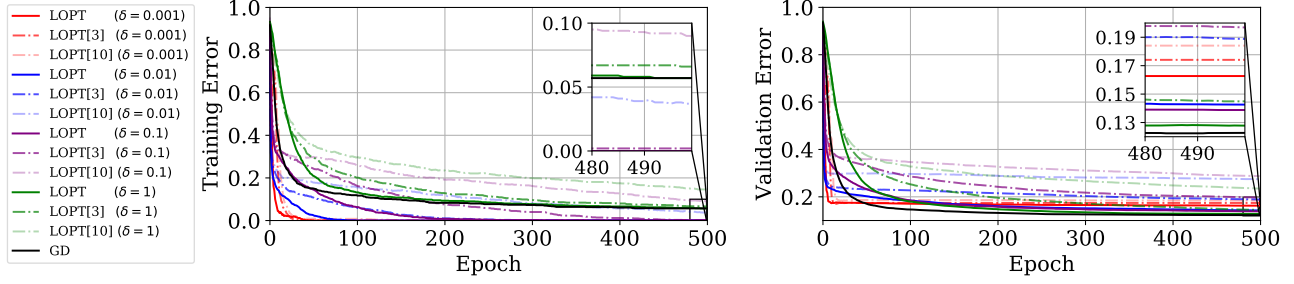


Figure 2: Training/Test Error of LanczosOPT/Gradient Descent (LOPT/GD) optimisers for Logistic Regression on the MNIST dataset with fixed learning rate $\alpha = 0.01$ across different damping values, δ . LOPT[η] denotes a modification to the LOPT that perturbs a subset of update directions by a factor of η (see Sec. 4.1 for details).

3.1 Adaptive updates, damping and the estimated curvature learning rate ratio

The learning rate in the flattest ($\lambda \approx 0$) directions is approximately $\frac{\alpha}{\delta}$, which is larger than that in the sharpest ($\lambda_i \gg \delta$) directions $\frac{\alpha}{\delta + \lambda_i}$. This difference in per direction effective learning rate makes the best possible (damped) loss reduction under the assumption that the loss function can be effectively modelled by a quadratic. Crucially, however, it is agnostic to how accurately each eigenvector component of the update estimates the true underlying loss surface, which is described in Theorem 1. Ignoring the gradient overlap with the eigenvectors $\phi_i \nabla L(\mathbf{w}_k)$ and assuming that the smallest eigenvalue $\lambda_P \ll \delta$, we see that $\mathcal{R}_{\text{est-curv}} = 1 + \frac{\lambda_1 - \lambda_P}{\delta}$. This is in contrast to SGD where $\mathbf{w}_{k+1} = \mathbf{w}_k - \sum_{i=1}^P \alpha \phi_i \phi_i^T \nabla L(\mathbf{w}_k)$ and hence $\mathcal{R}_{\text{est-curv}} = 1$.

The crucial point to note here is that the difference in $\mathcal{R}_{\text{est-curv}}$ is primarily controlled by the damping parameter: smaller values yield a larger $\mathcal{R}_{\text{est-curv}}$, skewing the parameter updates towards flatter directions. From Theorem 1 we see that overlap is reduced proportionally to the number of network parameters P and inversely to the number of samples taken for evaluation B , and so we expect the influence of this effect to become more significant for larger models (we show this to be the case in Sec. 5.1). In the next section we show that the damping parameter δ can be decomposed into a learning rate reduction term and a linear shrinkage of the curvature matrix.

3.2 Damping as an Approximate Linear Shrinkage

By re-writing the scaling applied in the direction of the i^{th} eigenvector, we note that:

$$\frac{1}{\lambda_i + \delta} = \frac{1}{\kappa(\beta\lambda_i + (1 - \beta))} \quad (3.3)$$

Solving gives us $\kappa = \frac{1}{\beta}$, $\beta = \frac{1}{1 + \delta}$. Hence, using a damping δ is equivalent to using a learning rate of

$\frac{\alpha}{\delta + 1}$ and applying a linear shrinkage factor $\frac{1}{1 + \delta}$ to the Hessian estimation. Thus larger damping corresponds to more aggressive shrinkage and hence the practice of *epsilon tuning* [20] can be viewed as approximate linear shrinkage. This idea that a combined estimator (such as linear shrinkage) can outperform the sample estimator is known as "Stein's Phenomenon" [44].

Optimality of Linear Shrinkage: Bun et al. [21] show that under the free multiplicative noise model, the linear shrinkage estimator

$$\tilde{\mathbf{H}} = \beta \mathbf{H} + (1 - \beta) \mathbf{I} = \arg \min_{\mathbf{H}^*} \|\mathbf{H} * - \mathbf{H}_{\text{true}}\|_{L2}$$

gives the minimum error between the estimator and the true covariance matrix. This implies that with an appropriately chosen shrinkage coefficient the optimiser more accurately descends the directions of the true risk, representing a bias variance trade-off. The empirical Hessian is all variance and no bias, whereas the identity is all bias and no variance, their combination reducing the mean square error. We expect an optimiser with well-tuned damping to perform better in validation and test set performance, which is the case in our experiments in 5. In practice we are not correcting the incorrect eigenvector directions, but simply the eigenvalues associated with those vectors. The practice of leaving the estimated eigenvectors unperturbed but shrinking the eigenspectrum, is well established and successfully applied in the field of sparse component analysis and finance [2].

4 Toy Example: MNIST

To validate our conjecture that movements in the sharp direction of the loss landscape are vital to generalisation, we first study a convex non stochastic example where we both explicitly and implicitly perturb the movement along the sharpest directions of the loss.

We implement a second-order optimiser based on the Lanczos iterative algorithm [17] (LanczosOPT). As a

δ	α		δ	α		
	0.0004	0.001		0.1	0.001	0.0001
1e-7	53.1 (62.9)		1e-1	6.7 (65.0)		
4e-4	21.1 (64.5)		1e-2		20.8 (64.8)	
1e-3	9.9 (63.5)	20.8 (64.4)	1e-3			48.2 (62.2)
5e-3		9.1 (66.2)	3e-4			527.2 (60.2)
8e-3		2.4 (65.8)	1e-4			711.3 (56.0)

Table 1: Spectral norm λ_1 at training end, in **bold**, with corresponding (validation accuracy). For learning rate/damping α, δ on CIFAR-100 using Adam (left) and KFAC (right) on the VGG-16.

baseline we also implement gradient descent (GD). We employ a training set of 1K MNIST [45] examples using Logistic Regression and validate on a held out test set of 10K examples.

4.1 LanczosOPT for Logistic Regression

The Lanczos Algorithm is an iterative algorithm for learning a subset of the eigenvalues/eigenvectors of any Hermitian matrix, requiring only matrix vector products. When the number of Lanczos steps, m , is significantly larger than the number of outliers, the outliers in the spectrum are estimated effectively [34]. Since the number of well-separated outliers from the spectral bulk is at most the number of classes [35] (which is $n_c = 10$ for this dataset), we expect the Lanczos algorithm to pick out these well-separated outliers when the number of iterations $k \gg n_c$ [34, 17] and therefore use $k = 50$. To investigate the impact of scaling steps in the Krylov subspace given by the sharpest directions, we consider the update \mathbf{w}_{k+1} of the form:

$$\mathbf{w}_k - \alpha \left(\sum_{i=1}^k \frac{1}{\lambda_i + \delta} \phi_i \phi_i^T \nabla L(\mathbf{w}_k) + \sum_{k+1}^P \frac{1}{\delta} \phi_i \phi_i^T \nabla L(\mathbf{w}_k) \right) \quad (4.1)$$

where $P = 7850$ (the number of model parameters) and hence the vast majority of “flat” directions remain unperturbed. For fixed α , δ controls the estimated curvature learning rate ratio.

Experimental Results: In Fig. 2, we observe evidence consistent with our central hypothesis: namely that as we increase $\mathcal{R}_{\text{est-curv}}$ (by decreasing the value of δ for a fixed α value of 0.01), the generalisation of the model suffers correspondingly.

To explore this effect in more detail, we introduce perturbations to the optimiser (denoted LOPT $[\eta]$), in which we scale up the eigenvalues in the denominator of Eqn. 4.1 by a factor of η (we explore scaling factors

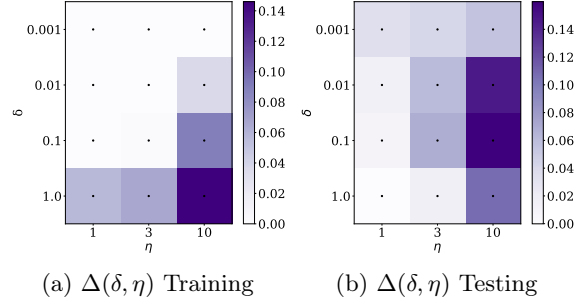


Figure 3: Error change with damping/sharp direction perturbation δ, η in LanczosOPT, relative to the single best run. Darker regions indicate higher error.

of 3 and 10). This explicitly reduces movement in sharp directions and consequently increases reliance on flat directions (which are left unperturbed). For each fixed value of δ , we see clearly that perturbations of greater magnitude cause greater harm to generalisation. Another interesting phenomenon we note is that for larger values of δ the perturbed optimisers suffer more gravely in terms of the effect on both training and validation. We visualise this in heat map form in Fig. 3, where we show the difference from the best training and testing error as a function of δ and η . We observe that the generalisation of all algorithms is worsened by explicit limitation of movement in the sharp directions (and an increase of estimated curvature learning rate ratio), however for extremely low damping measures (which are typical in adaptive optimiser settings) there is no or very minimal impact in training performance (upper region of Fig. 3 (a)).

5 Neural Networks: CIFAR100

To explore the conjecture for modern deep learning architectures for which running a large number of matrix vector products is less practical, we employ the second order optimiser KFAC [13] and Adam [6] on the VGG-16 [46] network on the CIFAR-100 [47] dataset. We specifically choose this network, as despite its size (over 16 million parameters) it can be effectively trained without batch-normalisation and weight decay and therefore allows us to isolate the effect of $\mathcal{R}_{\text{est-curv}}$, as opposed to the effect of different regularisation implementations for adaptive and non-adaptive methods as discussed by Loshchilov and Hutter [3] and Zhang et al. [27].

Both from a theoretical and practical perspective, it is beneficial to decay the learning rate. Whilst optimal asymptotic convergence guarantees are given for learning rates which decay proportionally to the square root of the number of iterations, or alternatively remain constant with a step size proportional to the inverse square

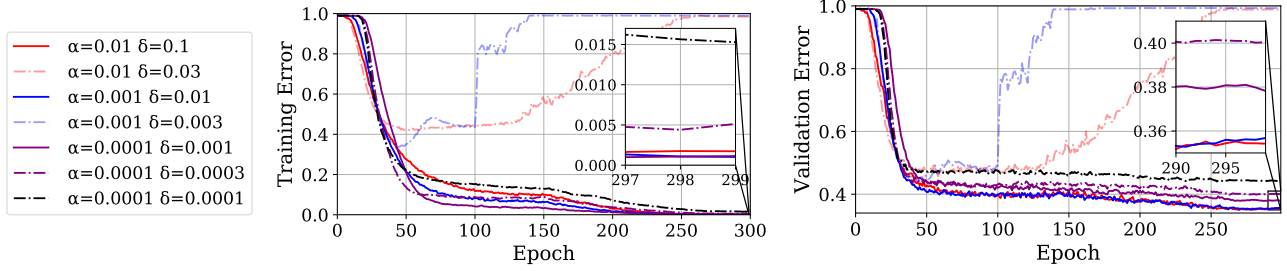


Figure 4: Training/Validation Error of the KFAC optimiser for the VGG-16 on the CIFAR-100 dataset with various learning rates α and damping values, δ .

root of the iteration number [48, 5], such aggressive decay rates or low learning rates are rarely employed in practice. Practitioners typically adopt a wide variety of schedules, with step scheduling amongst the most popular. Even though adaptive optimisation methods are less sensitive to the scheduling, convergence proofs require a learning rate reduction Reddi et al. [49] and in practice the performance without scheduling is significantly hampered. We use a linear schedule (detailed in suppl. material).

5.1 KFAC with VGG-16 on CIFAR-100

By decreasing the global learning rate α whilst keeping the damping to learning rate ratio $\kappa = \frac{\delta}{\alpha}$ constant, we reduce the estimated curvature learning rate ratio, $\mathcal{R}_{\text{est-curv}}$, which is determined by $\frac{\lambda_i}{\kappa\alpha} + 1$. In Fig. 4 we observe that as we increase $\mathcal{R}_{\text{est-curv}}$ the training performance is effectively unchanged, but generalisation suffers (65% \rightarrow 62.2%). Whilst decreasing the damping results in poor training for large learning rates (divergent trajectories in Fig. 4), for very low learning rates the network efficiently trains with a lower damping co-efficient. Such regimes further increase $\mathcal{R}_{\text{est-curv}}$ and we observe that they generalise more poorly. For $\alpha = 0.0001$ dropping the damping co-efficient δ from 0.0003 and 0.0001 drops the generalisation further to 60.2% and then 56% respectively. Similarly to Logistic Regression, for both cases the drop in generalisation is significantly larger than the drop in training accuracy.

Link to Solution Sharpness: Motivated by the literature on sharpness and generalisation from a Bayesian and minimum description length perspective [23] and the link between flatness and learning rates [50, 51], we investigate whether increasing $\mathcal{R}_{\text{est-curv}}$ is related to solution sharpness and show the results in Tab. 1. We see that increasing $\mathcal{R}_{\text{est-curv}}$ increases solution sharpness and decreases generalisation. As seen from the results where $\alpha = 0.0001$, this result is very prominent even for a fixed learning rate. The results of this experiment suggest that $\mathcal{R}_{\text{est-curv}}$ (rather than α alone [51]) has a significant influence on sharpness and generalisation in

second order methods. Our experiments on this network also suggest that the adaptive generalisation gap is prevalent even without alternative implementations of weight decay [3, 27] and hence this also is not the sole source of the adaptive generalisation gap. In fact as we shown in Sec 6, decoupled weight decay in combination with batch normalisation increases the movement along the sharpest directions, reducing $\mathcal{R}_{\text{est-curv}}$.

5.2 Adam with VGG-16 on CIFAR-100

We also employ the Adam optimiser on the same network and dataset for a variety of learning rate and damping coefficients as shown in Figure 5 and plot the results against the SGD baseline with maximal stable learning rate $\alpha = 0.01$ (corresponding to optimal performance). For the largest learning rate with which Adam trains ($\alpha = 0.0004$) with the standard damping coefficient $\delta = 10^{-8}$, we see that Adam significantly underperforms SGD, but that this gap is reduced by simply increasing the damping coefficient without harming performance. Over-damping decreases the performance.

For larger global learning rates enabled by a significantly larger than default damping parameter, when the damping is set too low, the training is unstable (corresponding to the dotted lines). Nevertheless, many of these curves with poor training out-perform the traditional setting on testing. We find that for larger damping co-efficients $\delta = 0.005, 0.0075$ Adam is able to match or even beat the SGD baseline, whilst converging faster. This evidences that for real problems of interest, adaptive methods may not be inherently worse than their non-adaptive counterparts as argued by Wilson et al. [9].

We note as shown in Table 1, that whilst decreasing δ always leads to smaller spectral norm, this does not always coincide with better generalisation performance. To investigate whether this alteration of δ could be widely applicable for deep learning practitioners, We run an experiment on VGG-16 using both batch normalisation [52] and decoupled weight decay [3]. We

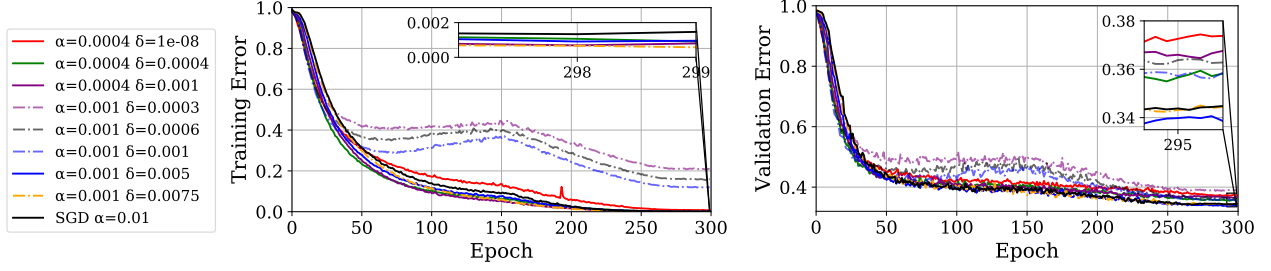


Figure 5: Training/Validation Error of the Adam optimiser for the VGG-16 on the CIFAR-100 dataset with various learning rates α and damping values, δ .

use a learning rate of 0.001 and a decoupled weight decay of $[0, 0.25]$. For this experiment (see appendix for training and validation curves) we observe that using a larger damping constant slightly assists training and improves generalisation, both without weight decay and with weight decay. This indicates that reducing $\mathcal{R}_{\text{est-curv}}$ using something as simple as increasing the damping constant δ could be beneficial in practice [20]. The spectral perturbation from the True Hessian (given in Theorem 1) is a function of the sampling noise. This is estimated in [33] and can be shown to change during training. This suggests that scheduling the damping constant δ could yield further performance improvements. Specifically Ledoit and Wolf [53] estimate the asymptotically optimal linear shrinkage using the dataset and Ledoit et al. [54] extend this to the non linear case which allows for outliers —we leave this to future work.

6 Prior work reduces reliance on flat directions.

In this section, we discuss how several recently introduced techniques for improving optimisation may relate to our conjecture. Let us consider the update equations for both SGD and Adaptive methods in the basis of the eigenvectors of the Hessian. We assume that the pre-conditioning matrix $\mathbf{B} \approx \mathbf{H}$. We also assume that $L2$ regularisation of magnitude γ is employed. The \mathbf{w}_{k+1} 'th weight vector is then given by:

$$\begin{cases} (1 - \gamma\alpha) \sum_i^P \phi_i \phi_i^T \mathbf{w}_k - \alpha \sum_i^P \phi_i^T \nabla L(\mathbf{w}) \phi_i & \text{SGD} \\ \sum_i^P (1 - \frac{\gamma\alpha}{\lambda_i + \delta}) \phi_i \phi_i^T \mathbf{w}_k - \alpha \sum_i^P \frac{\phi_i^T \nabla L(\mathbf{w})}{\lambda_i + \delta} \phi_i & \text{Adam} \end{cases} \quad (6.1)$$

where the damping δ is set to 10^{-8} in Adam. *Decoupled weight decay* [3] alters Adam such that the [weight decay update term](#)⁴ in Eqn 6.1 resembles that of SGD instead of that of Adam. This increases the weight decay along the sharpest directions of the loss which in turn increases the estimated curvature learning rate ratio in favour of these directions. To demonstrate this point,

⁴Colour is used to highlight the relevant terms in the formula.

consider the difference in channel weight vector direction $\hat{\mathbf{w}}_k$ [55] in the basis of the sharpest eigenvectors after one update of SGD $\sum_i^P \phi_i \phi_i^T (\hat{\mathbf{w}}_{k+1} - \hat{\mathbf{w}}_k)$:

$$\frac{-\eta(\mathbf{I} - \sum_i^P \phi_i \hat{\mathbf{w}}_k^T \nabla L(\hat{\mathbf{w}}_k) \phi_i^T \hat{\mathbf{w}}_k)}{\|\mathbf{w}_k\|^2}. \quad (6.2)$$

Hence decoupled weight decay, which by the [first term](#) in Equation 6.1 reduces the component along $\phi_i^T \hat{\mathbf{w}}_k$, through the reduction of the corrective term on the RHS of Eqn. 6.2, increases the effective learning rate. Padam [4], by changing the square root in the Adam update to an arbitrary power $p < 1/2$, increases both the weight decay and the [update in the sharp directions](#) in Equation 6.1), increasing the effective learning rate. Epsilon tuning [20], by increasing both ϵ and α increases both the [weight decay term](#) and [update in the direction of the sharpest eigenvectors term](#).

7 Conclusion

In this paper we show using the spiked covariance model that we expect sharp directions of the sampled loss surface to retain more information about the true loss surface compared to flatter directions. We show that for adaptive methods, which attempt to minimise the local quadratic of the sampled loss surface, that this leads to sub-optimal steps with worse generalisation performance. As a consequence, our framework gives a theoretical interpretation to several tried and tested techniques to improve adaptive gradient methods, such as decoupled weight decay, epsilon tuning and partial adaptivity, which we show are all methods which increase the movement along the sharpest directions in the loss surface. We further investigate the effect of damping on the solution sharpness and find that increasing damping always decreases the solution sharpness. We find that for large neural networks an increase in damping both assists training and is even able to best the SGD test baseline. An interesting consequence of this finding is that it suggests that damping should be considered an essential hyper-parameter in

adaptive gradient methods as it already is in stochastic second order methods.

References

- [1] Jinho Baik, Gérard Ben Arous, Sandrine Péché, et al. Phase transition of the largest eigenvalue for nonnull complex sample covariance matrices. *The Annals of Probability*, 33(5):1643–1697, 2005.
- [2] Joël Bun, Jean-Philippe Bouchaud, and Marc Potters. Cleaning large correlation matrices: tools from random matrix theory. *Physics Reports*, 666: 1–109, 2017.
- [3] Ilya Loshchilov and Frank Hutter. Decoupled weight decay regularization. 2019.
- [4] Jinghui Chen and Quanquan Gu. Closing the generalization gap of adaptive gradient methods in training deep neural networks. *arXiv preprint arXiv:1806.06763*, 2018.
- [5] Yurii Nesterov. *Introductory lectures on convex optimization: A basic course*, volume 87. Springer Science & Business Media, 2013.
- [6] Diederik P Kingma and Jimmy Ba. Adam: A method for stochastic optimization. *arXiv preprint arXiv:1412.6980*, 2014.
- [7] Matthew D Zeiler. Adadelta: an adaptive learning rate method. *arXiv preprint arXiv:1212.5701*, 2012.
- [8] Tijmen Tieleman and Geoffrey Hinton. Lecture 6.5-RMSProp: Divide the gradient by a running average of its recent magnitude. *COURSERA: Neural networks for machine learning*, 4(2):26–31, 2012.
- [9] Ashia C Wilson, Rebecca Roelofs, Mitchell Stern, Nati Srebro, and Benjamin Recht. The marginal value of adaptive gradient methods in machine learning. In *Advances in Neural Information Processing Systems*, pages 4148–4158, 2017.
- [10] Sangdoo Yun, Dongyoon Han, Seong Joon Oh, Sanghyuk Chun, Junsuk Choe, and Youngjoon Yoo. Cutmix: Regularization strategy to train strong classifiers with localizable features. *arXiv preprint arXiv:1905.04899*, 2019.
- [11] Qizhe Xie, Eduard Hovy, Minh-Thang Luong, and Quoc V. Le. Self-training with noisy student improves ImageNet classification, 2019.
- [12] Ekin D Cubuk, Barret Zoph, Jonathon Shlens, and Quoc V Le. Randaugment: Practical data augmentation with no separate search. *arXiv preprint arXiv:1909.13719*, 2019.
- [13] James Martens and Roger Grosse. Optimizing neural networks with Kronecker-factored approximate curvature. In *International conference on machine learning*, pages 2408–2417, 2015.
- [14] James Martens. New insights and perspectives on the natural gradient method. *arXiv preprint arXiv:1412.1193*, 2014.
- [15] Yann N Dauphin, Razvan Pascanu, Caglar Gulcehre, Kyunghyun Cho, Surya Ganguli, and Yoshua Bengio. Identifying and attacking the saddle point problem in high-dimensional non-convex optimization. In *Advances in neural information processing systems*, pages 2933–2941, 2014.
- [16] James Martens. Deep learning via Hessian-free optimization. In *ICML*, volume 27, pages 735–742, 2010.
- [17] Gérard Meurant and Zdeněk Strakoš. The Lanczos and conjugate gradient algorithms in finite precision arithmetic. *Acta Numerica*, 15:471–542, 2006.
- [18] Thomas George, César Laurent, Xavier Bouthillier, Nicolas Ballas, and Pascal Vincent. Fast approximate natural gradient descent in a Kronecker factored eigenbasis. In *Advances in Neural Information Processing Systems*, pages 9550–9560, 2018.
- [19] Magnus Tornstad. Evaluating the practicality of using a kronecker-factored approximate curvature matrix in newton’s method for optimization in neural networks, 2020.
- [20] Dami Choi, Christopher J Shallue, Zachary Nado, Jaehoon Lee, Chris J Maddison, and George E Dahl. On empirical comparisons of optimizers for deep learning. *arXiv preprint arXiv:1910.05446*, 2019.
- [21] Joël Bun, Romain Allez, Jean-Philippe Bouchaud, and Marc Potters. Rotational invariant estimator for general noisy matrices. *IEEE Transactions on Information Theory*, 62(12):7475–7490, 2016.
- [22] Stanislaw Jastrzebski, Maciej Szymczak, Stanislaw Fort, Devansh Arpit, Jacek Tabor, Kyunghyun Cho, and Krzysztof Geras. The break-even point on the optimization trajectories of deep neural networks. In *International Conference on Learning Representations*, 2020. URL <https://openreview.net/forum?id=r1g87C4KwB>.
- [23] Sepp Hochreiter and Jürgen Schmidhuber. Flat minima. *Neural Computation*, 9(1):1–42, 1997.
- [24] Yuanzhi Li, Colin Wei, and Tengyu Ma. Towards explaining the regularization effect of initial large learning rate in training neural networks. In *Advances in Neural Information Processing Systems*, pages 11674–11685, 2019.

- [25] Nitish Shirish Keskar and Richard Socher. Improving generalization performance by switching from Adam to SGD. *arXiv preprint arXiv:1712.07628*, 2017.
- [26] Dongruo Zhou, Yiqi Tang, Ziyang Yang, Yuan Cao, and Quanquan Gu. On the convergence of adaptive gradient methods for nonconvex optimization. *arXiv preprint arXiv:1808.05671*, 2018.
- [27] Guodong Zhang, Chaoqi Wang, Bowen Xu, and Roger Grosse. Three mechanisms of weight decay regularization. *arXiv preprint arXiv:1810.12281*, 2018.
- [28] Jinho Baik and Jack W Silverstein. Eigenvalues of large sample covariance matrices of spiked population models. *arXiv preprint math/0408165*, 2004.
- [29] Alex Bloemendal, Antti Knowles, Horng-Tzer Yau, and Jun Yin. On the principal components of sample covariance matrices. *Probability theory and related fields*, 164(1-2):459–552, 2016.
- [30] Richard Everson and Stephen Roberts. Inferring the eigenvalues of covariance matrices from limited, noisy data. *IEEE transactions on signal processing*, 48(7):2083–2091, 2000.
- [31] Joël Bun, Jean-Philippe Bouchaud, and Marc Potters. My beautiful laundrette: Cleaning correlation matrices for portfolio optimization, 2016.
- [32] Florent Benaych-Georges and Raj Rao Nadakuditi. The eigenvalues and eigenvectors of finite, low rank perturbations of large random matrices. *Advances in Mathematics*, 227(1):494–521, 2011.
- [33] Diego Granziol. Curvature is key: Sub-sampled loss surfaces and the implications for large batch training. *arXiv preprint arXiv:2006.09092*, 2020.
- [34] Diego Granziol, Xingchen Wan, and Timur Garipov. MLRG deep curvature. *arXiv preprint arXiv:1912.09656*, 2019.
- [35] Vardan Papayan. The full spectrum of deepnet Hessians at scale: Dynamics with SGD training and sample size. *arXiv preprint arXiv:1811.07062*, 2018.
- [36] Levent Sagun, Utku Evci, V Ugur Guney, Yann Dauphin, and Leon Bottou. Empirical analysis of the Hessian of over-parametrized neural networks. *arXiv preprint arXiv:1706.04454*, 2017.
- [37] Craig A Tracy and Harold Widom. Level-spacing distributions and the airy kernel. *Communications in Mathematical Physics*, 159(1):151–174, 1994.
- [38] Nouredine El Karoui et al. Tracy–Widom limit for the largest eigenvalue of a large class of complex sample covariance matrices. *The Annals of Probability*, 35(2):663–714, 2007.
- [39] Iain M Johnstone. On the distribution of the largest eigenvalue in principal components analysis. *Annals of statistics*, pages 295–327, 2001.
- [40] Guodong Zhang, Lala Li, Zachary Nado, James Martens, Sushant Sachdeva, George Dahl, Chris Shallue, and Roger B Grosse. Which algorithmic choices matter at which batch sizes? insights from a noisy quadratic model. In *Advances in Neural Information Processing Systems*, pages 8194–8205, 2019.
- [41] Stanislav Fort, Paweł Krzysztof Nowak, Stanisław Jastrzebski, and Srinu Narayanan. Stiffness: A new perspective on generalization in neural networks. *arXiv preprint arXiv:1901.09491*, 2019.
- [42] Liyuan Liu, Haoming Jiang, Pengcheng He, Weizhu Chen, Xiaodong Liu, Jianfeng Gao, and Jiawei Han. On the variance of the adaptive learning rate and beyond. *arXiv preprint arXiv:1908.03265*, 2019.
- [43] Hangfeng He and Weijie J Su. The local elasticity of neural networks. *arXiv preprint arXiv:1910.06943*, 2019.
- [44] Charles Stein. Inadmissibility of the usual estimator for the mean of a multivariate normal distribution. Technical report, Stanford University Stanford United States, 1956.
- [45] Yann LeCun. The MNIST database of handwritten digits. <http://yann.lecun.com/exdb/mnist/>, 1998.
- [46] Karen Simonyan and Andrew Zisserman. Very deep convolutional networks for large-scale image recognition. *arXiv preprint arXiv:1409.1556*, 2014.
- [47] Alex Krizhevsky, Geoffrey Hinton, et al. Learning multiple layers of features from tiny images. 2009.
- [48] John C Duchi. Introductory lectures on stochastic optimization. *The Mathematics of Data*, 25:99, 2018.
- [49] Sashank J Reddi, Satyen Kale, and Sanjiv Kumar. On the convergence of Adam and beyond. *arXiv preprint arXiv:1904.09237*, 2019.
- [50] Stanisław Jastrzebski, Zachary Kenton, Devansh Arpit, Nicolas Ballas, Asja Fischer, Yoshua Bengio, and Amos Storkey. Three factors influencing minima in SGD. *arXiv preprint arXiv:1711.04623*, 2017.
- [51] Lei Wu, Chao Ma, and E Weinan. How SGD selects the global minima in over-parameterized learning: A dynamical stability perspective. In *Advances in Neural Information Processing Systems*, pages 8279–8288, 2018.
- [52] Sergey Ioffe and Christian Szegedy. Batch normalization: Accelerating deep network training by

reducing internal covariate shift. *arXiv preprint arXiv:1502.03167*, 2015.

- [53] Olivier Ledoit and Michael Wolf. A well-conditioned estimator for large-dimensional covariance matrices. *Journal of multivariate analysis*, 88(2):365–411, 2004.
- [54] Olivier Ledoit, Michael Wolf, et al. Nonlinear shrinkage estimation of large-dimensional covariance matrices. *The Annals of Statistics*, 40(2):1024–1060, 2012.
- [55] Elad Hoffer, Ron Banner, Itay Golan, and Daniel Soudry. Norm matters: efficient and accurate normalization schemes in deep networks. In *Advances in Neural Information Processing Systems*, pages 2160–2170, 2018.
- [56] Gernot Akemann, Jinho Baik, and Philippe Di Francesco. *The Oxford handbook of random matrix theory*. Oxford University Press, 2011.
- [57] Pavel Izmailov, Dmitrii Podoprikin, Timur Garipov, Dmitry Vetrov, and Andrew Gordon Wilson. Averaging weights leads to wider optima and better generalization. *arXiv preprint arXiv:1803.05407*, 2018.

A Experiments with Batch Norm and Decoupled Weight Decay

In Fig. 6, we show that adapting epsilon for Adam in a network with batch normalisation and decoupled weight decay coefficient γ , the default for modern neural networks, also benefits from increasing the numerical stability or damping coefficient.

B Conditions for Theorem

For a fuller exposition of Theorem 1 in the main paper, we refer to [33] and [32]. However, the key tenet is that there is sufficient (but not full) independence between the elements of the noise matrix. Hence for the additive model the noise matrix converges to the semi-circle law. The work of [33] also develops a similar theorem for the multiplicative noise process under which the noise matrix converges to the Marcenko-Pastur distribution. We reproduce the technical conditions below for clarity.

To derive analytic results, we employ the Kolmogorov limit [2], where $P, B, N \rightarrow \infty$ but $\frac{P}{B} = q > 0$ and to account for dependence beyond the symmetry of the noise matrix elements, we introduce the σ -algebras $\mathfrak{F}^{(i,j)}$, and Lindeberg’s ratio $L_P(\tau)$, which are defined

for any $\tau > 0$ as follows:

$$\begin{aligned} \mathfrak{F}^{(i,j)} &:= \sigma\{\epsilon(\mathbf{w})_{kl} : 1 \leq k \leq l \leq P, (k, l) \neq (i, j)\}, \\ 1 \leq i \leq j \leq P \\ L_P(\tau) &:= \frac{1}{P^2} \sum_{i,j=1}^P \mathbb{E}|\epsilon(\mathbf{w})_{i,j}|^2 \mathbb{1}(|\epsilon(\mathbf{w})_{i,j}| > \tau) \end{aligned} \quad (\text{B.1})$$

Where $\epsilon(\mathbf{w})$ defines the matrix of fluctuations, which denotes the difference matrix between the true and empirical Hessians i.e.

$$\epsilon(\mathbf{w}) = \mathbf{H}_{\text{true}}(\mathbf{w}) - \mathbf{H}_{\text{emp}}(\mathbf{w}) \quad (\text{B.2})$$

Theorem 2. *The following technical conditions that in the limit $P \rightarrow \infty$, the limiting spectra density of $\epsilon(\mathbf{w})(\mathbf{w})$ is given by Wigner’s semi-circle law Akemann et al. [56]*

- i) $\frac{1}{P^2} \sum_{i,j=1}^P \mathbb{E}|\mathbb{E}(\epsilon(\mathbf{w})_{i,j}^2 | \mathfrak{F}^{i,j}) - \sigma_{i,j}^2| \rightarrow 0$,
- ii) $L_P(\tau) \rightarrow 0$ for any $\tau > 0$,
- iii) $\frac{1}{P} \sum_i |\frac{1}{P} \sum_{j=1}^P \sigma_{i,j}^2 - \sigma_e^2| \rightarrow 0$
- iv) $\max_{1 \leq i \leq P} \frac{1}{P} \sum_{j=1}^P \sigma_{i,j}^2 \leq C$

C Experimental Details

C.1 Lanczos Implementation

Due to its improved convergence properties [17], the Lanczos method can be viewed as an improved adaptation of the power iteration method, where the Krylov subspace $\mathcal{K}(\epsilon(\mathbf{w}), \mathbf{v}) = \text{span}\{\mathbf{v}, \epsilon(\mathbf{w})\mathbf{v}, \epsilon(\mathbf{w})^2\mathbf{v}, \dots\}$ is orthogonalised using the Gram-Schmidt procedure. The Conjugate Gradient algorithm, used in [16] can be derived from Lanczos [17].

To avoid calculating P Lanczos steps, we implement Equation 4.1 in the following manner

$$\mathbf{w}_k - \alpha \left(\sum_i^k \left(\frac{1}{\lambda_i + \delta} - \frac{1}{\delta} \right) \phi_i \phi_i^T \nabla L(\mathbf{w}_k) + \frac{\nabla L(\mathbf{w}_k)}{\delta} \right)$$

where the resolution of the identity can be used to show equivalence with Equation 4.1.

C.2 Learning Rate Schedule

For all experiments with VGG-16, we use a simple linear learning rate schedule used in [57]⁵:

$$\alpha_t = \begin{cases} \alpha_0, & \text{if } \frac{t}{T} \leq 0.5 \\ \alpha_0 \left[1 - \frac{(1-r)(\frac{t}{T} - 0.5)}{0.4} \right], & \text{if } 0.5 < \frac{t}{T} \leq 0.9 \\ \alpha_0 r, & \text{otherwise} \end{cases} \quad (\text{C.1})$$

⁵We found this to slightly outperform a “step” schedule of learning rate decays at fixed intervals.

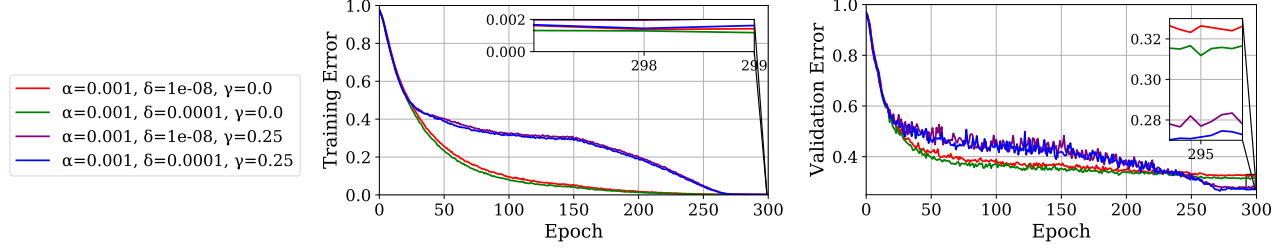


Figure 6: Training/Validation Error of the Adam optimiser for the VGG-16BN using Batch Normalisation and Decoupled Weight Decay on the CIFAR-100 dataset with various learning rates α and damping values, δ .

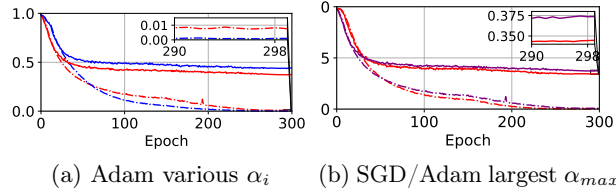


Figure 7: Training and Validation error for Adam/SGD on the VGG-16 & CIFAR-100 dataset with no weight decay or batch norm for various learning rates α_i , batch size $B = 128$. In Figure (a) the blue/red lines correspond to $\alpha = [0.0004, 0.0001]$ respectively and in Figure (b) the purple/red lines correspond to Adam/SGD respectively. Dashed lines indicate training performance and solid lines indicate validation performance.

where α_0 is the initial learning rate and t denotes the epoch. $T = 300$ is the total number of epochs budgeted for all CIFAR experiments. We set $r = 0.01$ for all experiments.